

Correlation properties of the maps of the NVSS survey and WMAP ILC

O.V. Verkhodanov^a, M.L. Khabibullina^a, E.K. Majorova^a, Yu.N. Parijskij^a

Special Astrophysical Observatory of the Russian AS, Nizhnij Arkhyz 369167, Russia

Received June 9, 2008; accepted June 30, 2008.

In this paper we study one-dimensional sections of the maps of WMAP ILC and of the NVSS survey on scale lengths of 0.75, 3, 4.5, and 6.75 degrees and analyze the correlation properties of the sections. On these maps we identify the domains where the absolute value of the correlation coefficient exceeds 0.5. The catalog of such domains is presented. It is shown that the number of the domains agrees with the number of such domains on simulated maps and this fact may be indicative of just statistical agreement of the arrangement of the domains considered.

PACS: 98.70.Dk, 98.70.Vc, 98.80.-k, 95.35.+d

1. INTRODUCTION

With the advent of high-precision millimeter-, centimeter-, and decimeter-wave radio-astronomical surveys it became possible to apply correlation studies to test the self-consistency of the cosmological models. The opening of public access to one-, three-, and five-year accumulated data on the measurements of cosmic microwave background (CMB) on the entire sky sphere [1, 2, 3, 4, 5, 6, 7] conducted using WMAP¹ (Wilkinson Microwave Anisotropy Probe) became a real breakthrough in this field. To reconstruct the CMB signal from multifrequency observations, it is used the method of inner linear combinations (ILC—Internal Linear Combination) of background components [1], which yielded a map of microwave background, also known as the ILC map, which is used to analyze low harmonics with multipole numbers $\ell \leq 100$. The ILC was constructed from observations made in five channels: 23 GHz (the K band), 33 GHz (the Ka band), 41 GHz (the Q band), 61 GHz (the V band), and 94 GHz (the W band).

Quite a few papers were devoted to analyzing the statistical properties of the signal in the reported ILC map and discussing the non-Gaussian nature of the data of this map revealed using various methods including phase analysis [8, 9, 10, 11], Maxwellian multipole vectors [12, 13], wavelets [14, 15, 16, 17], and Minkowski functionals [18, 19].

Non-Gaussian features extensively discussed by the researchers include the so-called Cold Spot (here-

after referred to as CS) with the size of about 10° (Galactic coordinates $l = 209^\circ$, $b = -57^\circ$) found in the distribution of cosmic microwave background in the Southern Hemisphere. The CS, which is statistically identified in the distribution of CMB, is one of the features of the map that are inconsistent with the hypothesis of uniform Gaussian background fluctuations. It was initially pointed out as a feature that deviates from Gaussian statistics when applying wavelet analysis [14, 20, 16, 17] to the data of the first and third years of observations of the WMAP mission.

A decrease of the space density of radio sources was found later in the NVSS maps [21], and this discovery led the researches to conclude that there must exist a giant 140-Mpc-large void at a redshift of $z < 1$, which produces the gravitational anomaly, which causes the integrated Sachs–Wolfe effect [22] and shows up as the CS. The researchers also discussed the possibility of explaining the spot in terms of the Sunyaev–Zel’dovich effect [23] due to the scattering in the Eridanus supergroup of galaxies [16, 24].

Exotic interpretations of the effect included the texture—a topological defect during the phase transition in the early Universe [25, 26] and Bianchi VII_h anisotropic cosmological model [27].

At the same time, serious arguments were advanced suggesting the map contains residual contribution of Galactic background components, which produces the observed deviation from the Gaussianity. This contribution can show up in the form of the earlier discovered relation between the cleaned mi-

¹ <http://lambda.gsfc.nasa.gov>

crowave background map and Galactic components of radiation [28, 29] and may also specify the properties of low-order multipoles $\ell \leq 20$, resulting in their unstable reconstruction [30]. In particular, these multipoles may explain the specific features of the CS, which demonstrate the deviation of the statistics of clusters of signal oscillation peaks in the vicinity of the spot [31]—the increase of the number of positive peaks.

An independent analysis of the spot's properties found in the region with close coordinates on maps and in radio-source counts in the NVSS survey [32] showed that the Cold Spot whose giant size and existence are difficult to explain in terms of the cosmological Λ CDM-model may be a common statistical deviation due to systematic effects [33].

In this paper we decided to verify the correlation properties of the NVSS and ILC maps on angular scales of 0.75, 3, 4.75, 6.75, and 9.75 degrees and to try to find and analyze CS type spots. We chose the angular scales to be much greater than the size of the smoothing window of the ILC map (1°), but smaller than 10° in order to preserve a sufficient number of pixels for statistical analysis. Our statistical analysis also included a sub-degree angular scale ($45' = 0.75^\circ$). In this paper we use the method of cross-correlation within selected sections proposed by Khabibullina et al. [34, 35] and employed to analyze low-frequency spatial fluctuations of microwave background in the domain covered by the RZF survey performed with the RATAN-600 radio telescope [36, 37]. To assess the results obtained, we simulated the maps by generating random Gaussian fluctuations with the power spectrum as implied by the Λ CDM cosmological model.

2. THE DATA

The ILC map bears the data on microwave background with a resolution of up to $\ell \leq 100$ (about 1°). This map was reconstructed based on multifrequency observations in five different wavelength intervals made over the entire celestial sphere and available from the web-site of the WMAP mission.

The NRAO VLA Sky Survey (NVSS) [32] is currently the most complete high-sensitivity and large-area survey in the Northern sky. It was performed with a VLA at a frequency of 1.4 GHz from 1993 until 1996 and covers the entire Northern sky above the declination of $\delta = -40^\circ$ (33884□ or 82% of the sky sphere). The survey is extensively used for various statistical cosmological studies. The catalog contains a total of 1.8×10^6 sources and, according to its description, is 99% and 50% complete down to the flux densities of $S_{1.4\text{ GHz}} = 3.5\text{ mJy}$ and 2.5 mJy , respec-

tively. The survey was made in the D-configuration of the VLA and the half-power size of the synthesized beam, which determines the resolution, was equal to about 45 arcsec. The data obtained as a result of the NVSS survey are available at the NRAO web-site², via the SkyView virtual telescope³, and from the CATS database⁴ [38, 39].

2.1. Properties of the NVSS catalog and the maps

We analyzed the maps of the NVSS survey by constructing one-dimensional sections with the smoothing due to the beam as described by Majorova [40]. Let us now consider two types of NVSS data: (1) the initial maps of the survey and (2) the catalog of radio sources. In second case, we also set the threshold for elimination of sources from the scans as a free parameter, thereby using the possibility of forming scans that are free of the influence of powerful radio sources.

To compare the sections constructed by different methods, we compute the correlation coefficients for: (1) scans based on the catalog and maps and (2) scans computed for two-dimensional maps and one-dimensional sections running through the center of the selected area.

In first case the correlation coefficient between all the sections exceeds 0.99, i.e., the sections computed based on catalog data and those based on the maps can be viewed as identical for our purposes, making our work much easier and allowing the source lists from the catalog to be used for the analysis. In latter case the correlation coefficient was 0.85 or higher, which we consider to be satisfactory and acceptable for fast computations and for the corresponding analysis.

To analyze the statistical correlation properties, we transformed the NVSS maps into a set of combined one-dimensional sections (M -scans) at given declinations with right ascensions ranging from 0^h to 24^h . We chose the declination step between the sections to be equal to the size of the chosen pixel on the sphere. The values in each pixel in modified one-dimensional NVSS sections are equal to the mean-squared source fluxes within the area of given size centered on the given pixel:

$$M_i = \frac{1}{N_r} \sum_{\kappa_i}^{N_r} S_{\kappa_i}^2, \quad P_{\kappa_i}(r) \in R_i, \quad (1)$$

² <http://www.cv.nrao.edu/nvss/>

³ <http://skyview.gsfc.nasa.gov>

⁴ <http://cats.sao.ru>

where N_r is the number of sources in the pixel (elementary sky area) of the given size of the NVSS survey; R_i is the pixel number i of given size; S_{κ_i} is the flux of the radio source number κ_i in pixel R_i , and $P_{\kappa_i}(r)$ is the position of source number κ_i . The pixel size R_i is specified by the correlation scale 0.75, 3, 4.5, 6.75, and 9.75°. Such a characterization of the NVSS map makes it possible to describe the distribution of sources in the given sky area, which varies from pixel to pixel and, in particular, allows statistical verification of the presence of hidden fluctuations due to the incompleteness of the WMAP catalog [2, 41, 42]. We exclude from our analysis the area in the NVSS survey at declinations $\delta < -40^\circ$ and the sections that cross it.

To produce sections of the ILC map we use the *mapcut* procedure of the GLESP package [43], which allows sections of the map to be made at the given declination with the given step in right ascension. Before performing this operation, we generated maps on the celestial sphere using the coefficients of spherical harmonics from the $a_{\ell m}$ set with the given resolution by applying the *cl2map* procedure from the same package with the function of map synthesis:

$$\Delta T(\theta, \phi) = \sum_{\ell}^{\ell_{max}} \sum_{m=1}^{\ell} (a_{\ell, m} Y_{\ell, m}(\theta, \phi) + a_{\ell, -m} Y_{\ell, -m}(\theta, \phi)), \quad (2)$$

where $Y_{\ell, m}$ are the spherical functions; ℓ is the number of the multipole; m is the mode of the multipole ℓ ; (θ, ϕ) are the polar coordinates, and $a_{\ell, m}$ are the coefficients of spherical harmonics satisfying the following condition:

$$Y_{\ell, -m}(\theta, \phi) = (-1)^m Y_{\ell, m}^*(\theta, \phi), \\ a_{\ell, m} = (-1)^m a_{\ell, -m}^*. \quad (3)$$

3. CORRELATION ANALYSIS

The adopted approach is based on a two-steps one-dimensional correlation analysis between the M scans of the NVSS and the sections of the ILC map performed in order to search for correlation features on various scales.

At the first stage we selected correlated scans of these two maps and identified the cases where the level of correlations was higher than the average level estimated from simulated records (Fig. 1). Although such a low correlation level makes the concept of correlation between the scans sounds problematic, we nevertheless took into account the fact that small-scale correlations, if present, must show up above the Gaussian noise and rise the correlation level K above the statistically expected value.

We use standard method to compute the correlation coefficients K_t for one-dimensional sections:

$$K_t = \frac{\text{cov}(x_{ILC, t}, x_{NVSS, t})}{\sigma_{ILC, t} \sigma_{NVSS, t}} \\ = \frac{\sum_{i=1}^n (x_{i, ILC, t} - \overline{x_{ILC, t}})(x_{i, NVSS, t} - \overline{x_{NVSS, t}})}{\sigma_{ILC, t} \sigma_{NVSS, t}}, \quad (4)$$

where $x_{i, ILC, t}$ is i th element of the one-dimensional section of the ILC map written in the form of vector $x_{ILC, t}$ for the given scale or coordinate interval t ; $x_{i, NVSS, t}$ is the similar quantity, where vector $x_{NVSS, t}$ is based not on a section of the ILC map, but on the M scan of NVSS computed by formula (1); $\overline{x_{ILC, t}}$ and $\overline{x_{fgd, t}}$ are the data vectors for the sections of the ILC maps and M sections of NVSS respectively and $\sigma_{ILC, t}$ and $\sigma_{NVSS, t}$ are the corresponding variances.

The second stage consisted in analyzing the properties of the selected sections in order to search for intervals with correlation coefficients $|K| \geq 0.5$. Let us point out from the start that if the procedure involves few points, correlations between the M -sections and NVSS data can always be found even in two random records. Our simulation of pure Gaussian noise using procedure *fpatt* of the FDPS reduction system [44, 45] showed that the optimum number of counts such that the correlation coefficient for two random records is $|K| < 0.5$ should be no less than 26. We adopted this number of counts as our minimum interval in pixels to search for significant correlations ($|K| \geq 0.5$) in the records selected at the first stage. Figure 2 shows an example of such a record, which contains an interval with $|K| \geq 0.5$.

4. RESULTS

Due to the insufficient number of pixels in scans we did not use the data on for angular scales 9.75° and thus excluded regions with the sizes on the order of that of the Cold Spot. We analyze the sections and maps, constructed for the angular scales of 0.75, 3, 4.5, and 6.75°. Tables 1–4 list the central coordinates of the intervals and the correlation coefficients.

The number of events with $K \leq -0.5$ (34 of 53, 19 of 34, 7 of 10, and 7 of 13 for the angular scales of 0.75, 3, 4.5, and 6.75° respectively) exceeds a bit the number of events with $K \geq 0.5$. This result could be explained by invoking the Sachs–Wolfe effect however, our subsequent statistical simulation shows that such deviations are within the limits of Gaussian scatter.

To test the statistical significance of the results with the Monte Carlo technique we used GLESP

Table 1: Coordinates of the centers of the areas with the correlation coefficients $|K| \geq 0.5$. The coordinates: right ascension α in hours and declination δ in degrees (for the epoch of 2000.0) are accurate to about half the pixel size. The size of the pixel side is 0.75°

α^h	δ°	k	α^h	δ°	k	α^h	δ°	k
14.407	-32.87	-0.58	8.387	12.12	0.52	6.024	45.12	-0.55
12.332	-37.37	-0.52	21.711	13.62	-0.52	7.228	45.12	-0.62
12.647	-37.37	-0.52	3.431	15.88	0.52	7.413	52.62	-0.50
12.961	-37.37	-0.59	3.535	15.88	0.51	9.472	52.62	-0.57
10.002	-32.87	-0.50	3.639	15.88	0.55	18.203	52.62	-0.59
6.747	-29.87	0.64	3.795	15.88	0.51	18.054	57.12	-0.54
11.517	-16.37	-0.54	7.342	30.12	-0.56	23.120	57.12	-0.50
11.726	-16.37	-0.56	17.805	30.12	-0.52	22.379	59.38	0.50
18.969	-16.37	-0.57	17.920	30.12	-0.65	1.104	60.12	0.55
7.574	-10.37	-0.52	22.719	30.12	-0.51	5.931	62.38	-0.51
7.726	-10.37	-0.50	0.716	33.12	-0.52	6.245	63.88	0.52
0.700	-1.38	0.51	11.001	36.88	0.59	8.454	71.38	-0.57
3.751	-1.38	0.56	14.313	36.88	0.51	9.550	71.38	-0.55
5.402	-1.38	-0.51	14.938	36.88	0.53	9.863	71.38	-0.51
5.702	-1.38	-0.51	3.508	38.38	-0.51	12.698	78.88	0.53
2.313	6.12	0.59	19.006	38.38	-0.55	13.734	78.88	0.64
3.938	12.12	0.51	4.864	41.38	-0.50	1.169	82.62	-0.62
8.080	12.12	0.52	5.464	41.38	-0.52			

Table 2: Coordinates of the centers of the areas with the correlation coefficients $|K| \geq 0.5$. The coordinates: right ascension α in hours and declination δ in degrees (for the epoch of 2000.0) are accurate to about half the pixel size. The size of the pixel side is 3°

α^h	δ°	k	α^h	δ°	k	α^h	δ°	k
23.448	-35.88	0.57	3.451	9.88	-0.54	8.207	25.62	-0.63
0.807	-7.38	-0.60	12.586	9.88	-0.51	9.538	25.62	-0.51
11.293	-7.38	-0.57	2.271	14.38	0.51	22.625	25.62	-0.54
14.117	-7.38	-0.63	16.724	14.38	0.63	3.931	30.12	-0.56
16.133	-7.38	-0.56	20.027	14.38	0.53	15.724	30.12	-0.53
23.595	-7.38	-0.52	21.885	14.38	0.55	21.871	40.62	-0.61
6.820	-4.38	0.53	3.397	19.62	-0.55	1.984	45.12	0.53
21.061	-4.38	0.51	6.158	19.62	-0.55	4.535	45.12	0.57
8.206	-2.12	0.51	8.281	19.62	-0.51	5.953	45.12	0.52
0.800	-1.38	0.53	2.787	21.12	-0.51	2.965	66.12	0.52
0.800	-0.62	0.52	3.645	21.12	-0.59			
19.400	0.12	0.55	8.405	21.88	-0.66			

Table 3: Coordinates of the centers of the areas with the correlation coefficients $|K| \geq 0.5$. The coordinates: right ascension α in hours and declination δ in degrees (for the epoch of 2000.0) are accurate to about half the pixel size. The size of the pixel side is 4.5°

α^h	δ°	k	α^h	δ°	k	α^h	δ°	k
21.608	-32.12	0.52	15.218	18.88	-0.52	22.444	35.38	-0.51
12.300	0.12	-0.50	16.925	35.38	-0.50	23.213	57.12	0.57
22.500	0.12	0.55	18.764	35.38	-0.55			
13.950	18.88	-0.57	21.708	35.38	-0.51			

Table 4: Coordinates of the centers of the areas with the correlation coefficients $|K| \geq 0.5$. The coordinates: right ascension α in hours and declination δ in degrees (for the epoch of 2000.0) are accurate to about half the pixel size. The size of the pixel side is 6.75°

α^h	δ°	k	α^h	δ°	k	α^h	δ°	k
5.258	-39.62	-0.52	21.660	-17.12	0.52	12.155	31.62	0.73
10.516	-39.62	-0.54	1.812	-6.62	0.54	17.406	43.62	0.66
12.269	-39.62	-0.50	14.617	9.88	-0.60	7.039	54.88	0.52
10.904	-34.38	-0.55	0.478	19.62	-0.58			
0.942	-17.12	0.68	3.822	19.62	-0.57			

Table 5: The number of events where the correlation coefficient exceeds $K = 0.5$ in the “ILC–NVSS” scans and in the average coefficient inferred from simulated data. The estimates are made in the scans with the same declination

Angular scale, degrees	Number of “ILC–NVSS” events	Average number of “model–NVSS” events
0.75	53	51.2 ± 12.1
3.0	34	22.1 ± 6.0
4.5	10	20.0 ± 6.1
6.75	13	15.3 ± 5.4

package [47] to generate 50 simulated random maps of microwave background for different angular scales with a power spectrum corresponding to Λ CDM cosmology. We constructed our maps with pixelization on different angular scales similar to the pixelization of the maps studied. On each map we identified the scans at the declinations listed in the previous table and computed the number of events with the correlation coefficient $|K| \geq 0.5$. We list the computed number of events in Table 5.

The results listed in Table 5 indicate that no statistically significant deviations can be found between the NVSS map—ILC CMB map correlation and the NVSS map—random CMB maps correlation on angular scales of $(1-7)^\circ$. However, we identified the domains listed in the catalog (Tables 1–4), where the behavior of M -scans resembles that of CMB. It is not improbable that the correlation between the positions of some spots from the catalog of celestial areas may be due to a real physical effect, although we would rather conclude that most of the correlated (anticorrelated) spots (or perhaps even all spots) can be explained as simple statistical coincidences.

5. CONCLUSIONS

We performed a correlation analysis of the CMB maps and of the modified NVSS map smoothed at different angular scales using the method of one-dimensional sections. We constructed the modified NVSS map using the distribution of the mean squared flux of sources within an area of given size centered on the

pixel specified by the selected area. We used the data obtained as a result of our search for correlations to catalog the regions with $|K| \geq 0.5$ at various angular scales. We simulated the CMB maps using the Monte Carlo method and the angular power spectrum of the Λ CDM cosmology as our input parameter. We performed a similar correlation analysis for 50 generated CMB models. We found that the statistical properties of the correlations on the angular scales studied ($0.75, 3, 4.5,$ and 6.75°) does not differ from those of random maps. This result leads us to conclude that the correlations found may be due to statistical coincidence. However, it is of interest to perform two-dimensional correlation pixelization (mapping) of the sky using catalogs for other wavelength intervals. We plan to perform such an analysis in our next paper. We are going to, in particular, to look for the Sachs–Wolfe effect.

Acknowledgments. We are grateful to NASA for making available their NASA Legacy Archive, from where we adopted WMAP data. We are also grateful to the authors of HEALPix for the use of their ⁵ package [46], which we used to transform WMAP maps into the coefficients $a_{\ell m}$. In this paper we used the GLESP ⁶ package [47, 43] for subsequent analysis of the CMB data on the sphere and the FADPS system ⁷ for the reduction of one-dimensional data [44, 45]. This work was supported in part by the

⁵ <http://www.eso.org/science/healpix/>

⁶ <http://www.glesp.nbi.dk>

⁷ http://sed.sao.ru/~vo/fadps_e.html

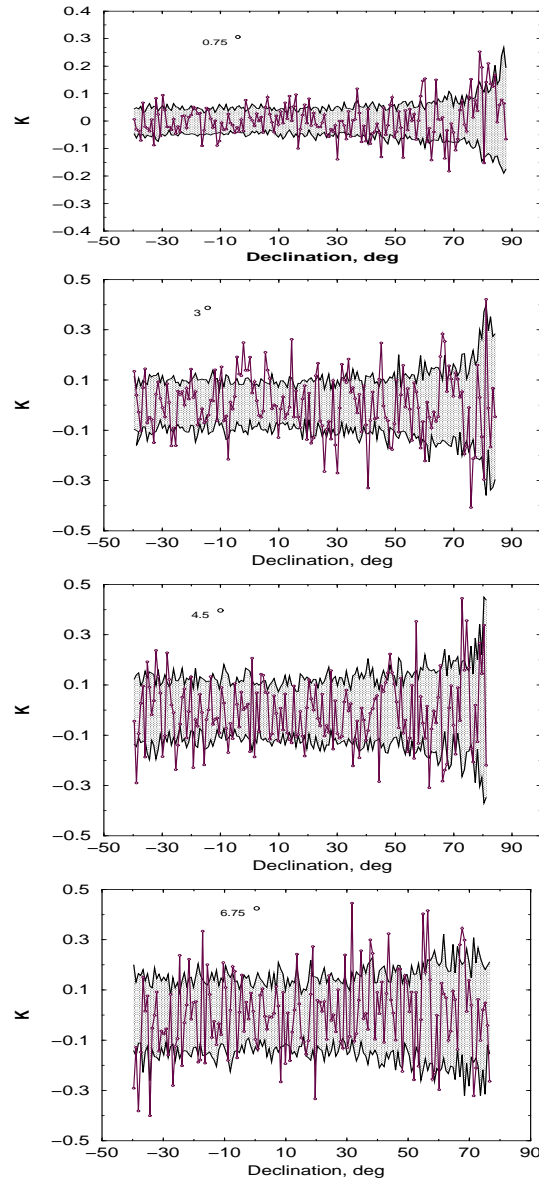


Figure 1: Correlation coefficients for different angular scales as a function of declination δ . The correlation scales (0.75, 3, 4.5, and 6.75 degrees) are indicated in the figures. Gray shade shows the allowable level of cross correlations as computed based on the data for 50 simulated maps for Λ CDM cosmology.

grant “Leading scientific schools of Russia”. O.V.V. acknowledges partial support from the Russian Foundation Basic Research for partial support of the work (grant no. 08-02-00159) and Russian Foundation for Domestic Science Support.

References

- C. L. Bennett, M. Halpern, G. Hinshaw, et al., *Astrophys. J. Supp.* **148**, 1 (2003), astro-ph/0302207
- C. L. Bennett, R. S. Hill, G. Hinshaw, et al., *Astrophys. J. Supp.* **148**, 97 (2003), astro-ph/0302208
- D. N. Spergel, L. Verde, H. V. Peiris, et al., *Astrophys. J. Supp.* **148**, 175 (2003), astro-ph/0302209
- G. Hinshaw, D. N. Spergel, L. Verde, et al., *Astrophys. J. Supp.* **170**, 288 (2007), astro-ph/0603451
- D. N. Spergel et al., *Astrophys. J. Supp.* **170**, 377 (2007), astro-ph/0603449
- G. Hinshaw, J. L. Weiland, R. S. Hill, et al., *Astrophys. J. Supp.*, submitted, (2008), arXiv:0803.0732
- E. Komatsu, J. Dunkley, M. R.olta, et al., *Astrophys. J. Supp.*, submitted, (2008), arXiv:0803.0547
- L.-Y. Chiang, P. D. Naselsky, O. V. Verkhodanov, and M. J. Way, *Astrophys. J.* **590**, L65 (2003), astro-ph/0303643
- P. D. Naselsky, A. G. Doroshkevich, and O. V. Verkhodanov, *Astrophys. J. Supp.* **148**, 175 (2003), astro-ph/0302209

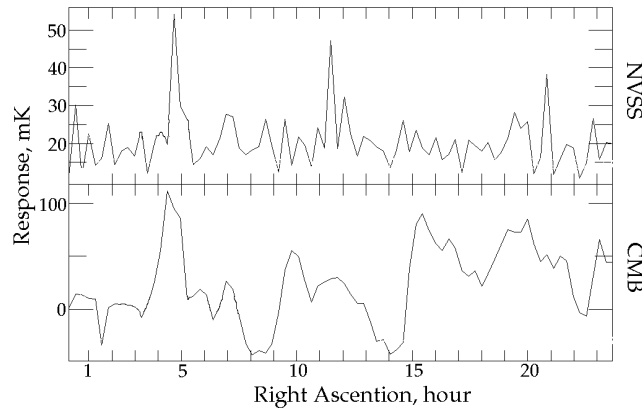


Figure 2: Examples of NVSS (upper plot) and CMB (WMAP ILC) (lower plot) sections at 4.5-degree intervals, where the correlation coefficient $|K| \geq 0.5$.

- danov, *Astrophys. J* **599**, L53 (2003), astro-ph/0310542
- P. D. Naselsky, A. G. Doroshkevich, and O. V. Verkhodanov, *MNRAS* **349**, 695 (2004), astro-ph/0310601
- P. Coles, P. Dineen, J. Earl, and D. Wright, *MNRAS* **350**, 989 (2004), astro-ph/0310252
- C. J. Copi, D. Huterer, and G. D. Starkman *Phys. Rev. D* **70**, 043515 (2004), astro-ph/0310511
- C. J. Copi, D. Huterer, D. J. Schwarz, and G. Starkman, *Phys. Rev. D* **75**, 023507 (2007), astro-ph/0605135
- P. Vielva, E. Martinez-Gonzalez, R. B. Barreiro, et al., *Astrophys. J* **609**, 22 (2004), astro-ph/0310273
- P. Mukherjee and Y. Wang, *Astrophys. J* **613**, 51 (2004).
- M. Cruz, E. Martinez-Gonzalez, P. Vielva, and L. Cayon, *MNRAS* **356**, 29 (2005).
- M. Cruz, L. Cayon, E. Martinez-Gonzalez, et al., *Astrophys. J* **655**, 11 (2007), astro-ph/0603859
- H. K. Eriksen, D. I. Novikov, P. B. Lilje, et al., *Astrophys. J* **612**, 64 (2004).
- C.-G. Park, C. Park, and J. R. Gott III, *Astrophys. J* **660**, 959 (2006), astro-ph/0608129
- L. Cayon, J. Jin, and A. Treaster, *MNRAS* **362**, 826 (2005).
- L. Rudnick, S. Brown, and L. R. Williams, *Astrophys. J* **671**, 40 (2007), arXiv:0704.0908
- R. K. Sachs and A. M. Wolfe, *Astrophys. J* **147**, 73 (1967).
- R. A. Sunyaev and Ya. B. Zeldovich, *Astrophys. Sp. Sci.* **7**, 3 (1970).
- S. Brough, D. A. Forbes, V. A. Kilborn, et al., *MNRAS*, **369**, 1351 (2006).
- M. Cruz, N. Turok, P. Vielva, et al., *Science* **318**, 1612 (2007), arXiv:0710.5737
- M. Cruz, E. Martinez-Gonzalez, P. Vielva, et al., (2008), arXiv:0804.2904
- T. Jaffe, A. J. Banday, H. K. Eriksen, et al., *Astrophys. J* 629, L1, 2005 (astro-ph/0503213)
- P. D. Naselsky and O. V. Verkhodanov, *Int. J. Mod. Phys. D* **17**, 179 (2008), astro-ph/0609409
- P. D. Naselsky and O. V. Verkhodanov, *Astrophys. Bull.* **62**, 218 (2007).
- P. D. Naselsky, O. V. Verkhodanov, and M. T. B. Nielsen, *Astrophys. Bull.* **63**, 216 (2008), arXiv:0707.1484
- P. D. Naselsky, P. R. Christensen, P. Coles, et al., (2007), arXiv:0712.1118
- J. J. Condon, W. D. Cotton, E. W. Greisen, et al., *AJ* **115**, 1693 (1998).
- K. M. Smith and D. Huterer, (2008), arXiv:0805.2751
- M. L. Khabibullina, O. V. Verkhodanov, and Yu. N. Parijskij, *Astrophys. Bull.* **63**, 95 (2008).
- M. L. Khabibullina, O. V. Verkhodanov, and Yu. N. Parijskij, in *Practical Cosmology, V.II. Proceedings of the International Conf. "Problems of Practical Cosmology"*, Ed. by Yu. Baryshev, I.N. Taganov, P. Teerikorpi (Russian Geographic Soc., St. Petersburg, 2008), p. 206.
- Yu. N. Parijskij, N. N. Bursov, A. B. Berlin, et al., *Gravitation & Cosmology* **10**, 139 (2005), astro-ph/0508065
- N. N. Bursov, Yu. N. Pariiskii, E. K. Maiorova, et al., *Astron. Rep.* **51**, 197 (2007).
- O. V. Verkhodanov, S. A. Trushkin, H. Andernach, and V. N. Chernenkov, in *Astronomical Data Analysis Software and Systems VI*, Ed. by G.Hunt and H.E.Payne, ASP Conf. Ser., **125**, 322 (1997), astro-ph/9607104
- O. V. Verkhodanov, S. A. Trushkin, H. Andernach, and V. N. Chernenkov, *Bull. Spec. Astrophys. Obs.* **58**, 118 (2005), arXiv:0705.2959
- E. K. Majorova, *Astrophys. Bull.* **63**, 56 (2008).
- E. L. Wright, X. Chen, N. Odegard, et al., *Astrophys. J. Supp.*, submitted (2008), arXiv:0803.0577
- S. A. Trushkin, *Bull. Spec. Astrophys. Obs.* **55**, 90 (2003).
- O. V. Verkhodanov, A. G. Doroshkevich, P. D. Naselsky, et al., *Bull. Spec. Astrophys. Obs.* **58**, 40 (2005).
- O. V. Verkhodanov, in *Astronomical Data Analysis Software and Systems VI*, Ed. by G.Hunt and H.E.Payne,

- ASP Conf. Ser. **125**, 46 (1997).
- O. V. Verkhodanov, B. L. Erukhimov, M. L. Monosov, et al., *Bull. Spec. Astrophys. Obs.* **36**, 132 (1993).
- K. Górski, E. Hivon, A. J. Banday, et al., *Astrophys. J* **622**, 759 (2005).
- A. G. Doroshkevich, P. D. Naselsky, O. V. Verkhodanov et al., *Int. J. Mod. Phys. D* **14**, 275 (2003), [astro-ph/0305537](#)